Electronic Supplementary Material (ESI) for Materials Chemistry Frontiers.

Eletronic Supplementary Information for "Tuning conduction band position in Ga-doped (Cd,Zn)S contact layers for photovoltaics"

Lauryn L. Baranowski,[*,†,‡] Steven Christensen,[†] Adam W. Welch,[†,‡] Stephan Lany,[†] Matthew Young,[†] Eric S. Toberer,[‡] and Andriy Zakutayev[*,†]

†*National Renewable Energy Laboratory, Golden, CO 80401 USA*

‡*Colorado School of Mines, Golden, CO 80401 USA*

E-mail: l.l.baranowski@gmail.com; andriy.zakutayev@nrel.gov

Table S1: ALD cycles and resultant film thicknesses for $Cd_{1-x}Zn_xS$ samples.

Composition	Cycles	Thickness (nm)
CdS	727x DMCd	90.8
$Cd_{0.90}Zn_{0.10}S$	68x {1x DEZ - 9x DMCd}	83.8
$Cd_{0.61}Zn_{0.39}S$	297x {1x DEZ - 1x DMCd}	85.0
$Cd_{0.14}Zn_{0.86}S$	52x {9x DEZ - 1x DMCd}	73.7

Table S2: Device data (open curcuit voltage, short circuit current, fill factor, and efficiency) corresponding to devices shown in Fig. S3.

Contact layer	V_{OC} (V)	J_{SC} (mA/cm^2)	FF	Eff (%)
CBD CdS	0.392	3.18	33.3	0.416
ALD CdS	0.362	5.28	41.7	0.796
$Cd_{0.90}Zn_{0.10}S$	0.265	2.48	31.2	0.205
$Cd_{0.61}Zn_{0.39}S$	0.0001	0.00329	0	0
$Cd_{0.14}Zn_{0.86}S$	0.00627	0.11192	0	0

Table S3: Device data (open curcuit voltage, short circuit current, fill factor, and efficiency) corresponding to devices shown in Fig. 7.

Contact layer	V_{OC} (V)	J_{SC} (mA/cm^2)	FF	Eff (%)
CBD CdS	0.211	3.82	40.8	0.329
Undoped $Cd_{0.6}Zn_{0.4}S$	0.00047	0.03256	0	0
2.4% Ga-doped $Cd_{0.6}Zn_{0.4}S$	0.306	4.40	27.5	0.370
3.6% Ga-doped $Cd_{0.6}Zn_{0.4}S$	0.305	5.32	29.8	0.484
5.5 % Ga-doped $Cd_{0.6}Zn_{0.4}S$	0.449	6.24	32.9	0.920

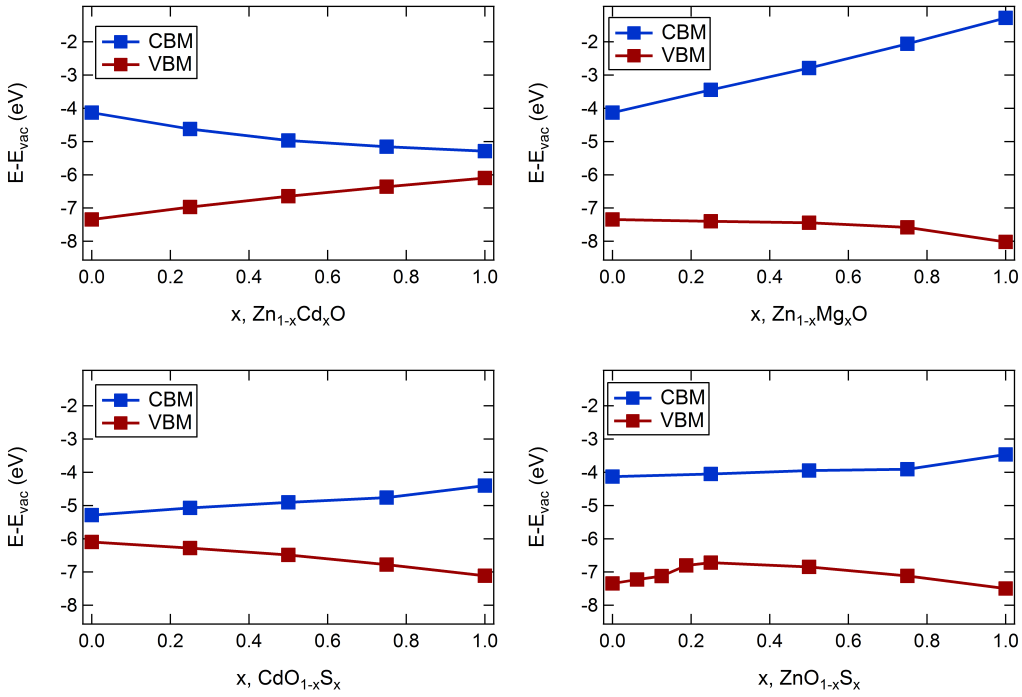

Figure S1: DFT calculations of VBM and CBM tuning for other alloy systems that were considered as contact layer candidates.

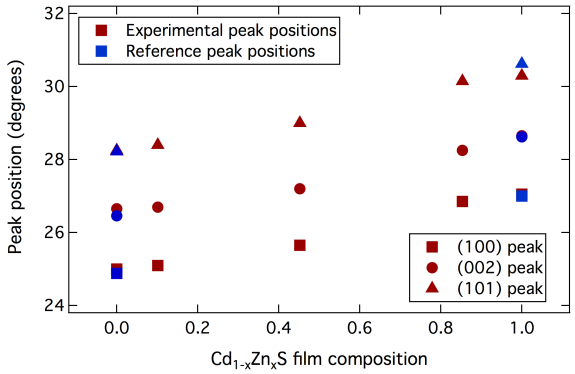

Figure S2: XRD peak shifts due to addition of Zn into the CdS hexagonal wurtzite structure, demonstrating true alloying.

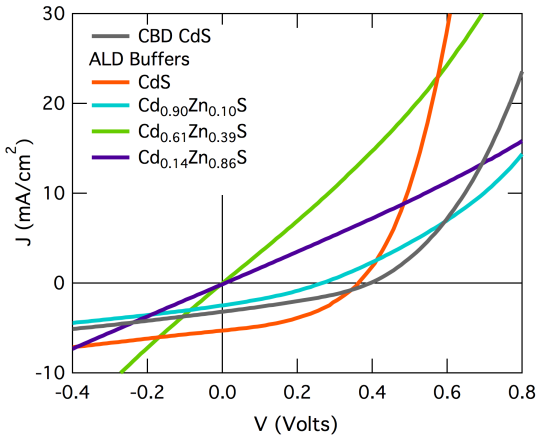

Figure S3: JV characterization of $CuSbS_2$ devices with different $Cd_{1-x}Zn_xS$ contact layers, compared to a reference cell with a CBD CdS contact layer (device metrics shown in Table S2).

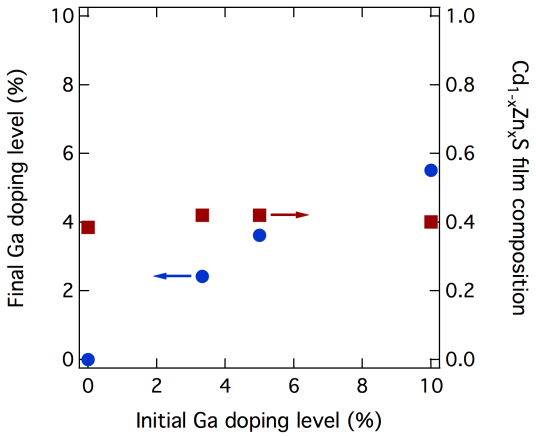

Figure S4: The Ga-doped films had varying levels of final Ga concentration, while maintaining the $Cd_{0.6}Zn_{0.4}S$ base composition.

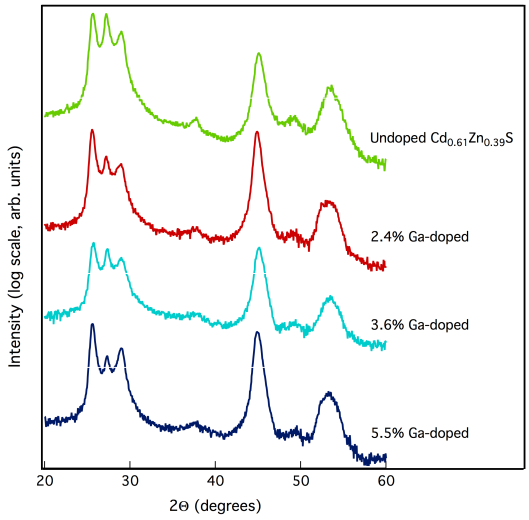

Figure S5: Ga-doping did not affect the overall wurtzite structure of the base $Cd_{0.6}Zn_{0.4}S$ compound.

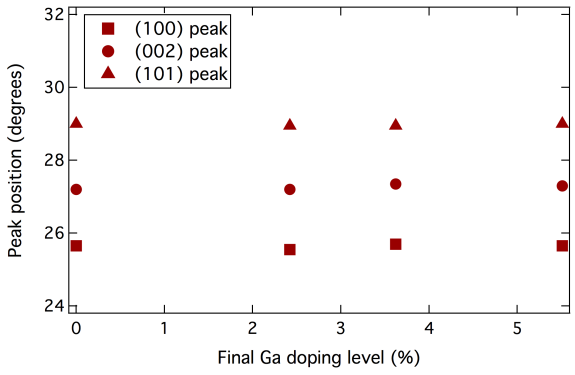

Figure S6: As shown in Fig. S5, we did not observe peak shifts in the XRD patterns with increased Ga-doping.

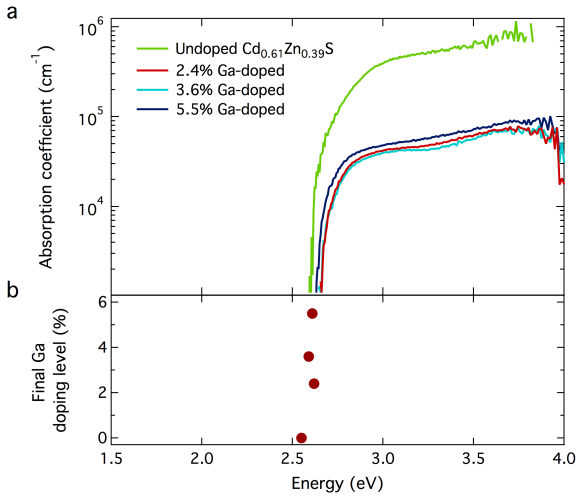

Figure S7: No changes in optical absorption onset were observed at different levels of Ga-doping in $Cd_{0.6}Zn_{0.4}S$.

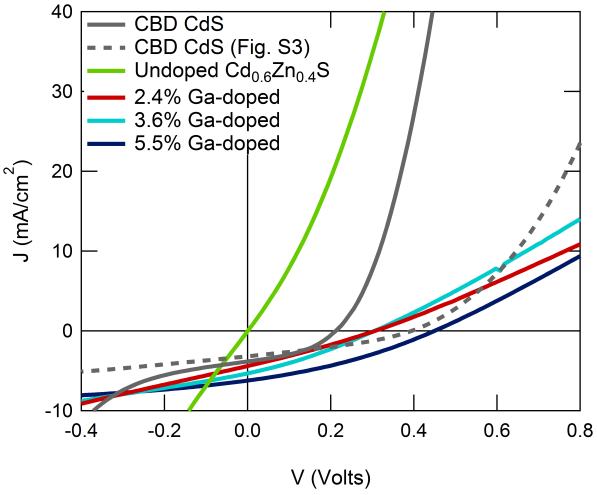

Figure S8: Current-voltage data for $CuSbS_2$ devices with $Cd_{0.6}Zn_{0.4}S$ contact layers. Increased levels of Ga-doping resulted in significant increases in the open circuit voltage from the reference CdS contact layer, although overall device efficiency remained low. Device metrics can be found in Table S3. Note that we also show the CBD CdS device from Fig. S3, which showed higher performance. However, the device from Fig. S3 is made with a different underlying $CuSbS_2$ absorber than all other devices shown in this figure. As such, this emphasizes why it was important to only compare device performance within a given sample set made from the same $CuSbS_2$ absorber.

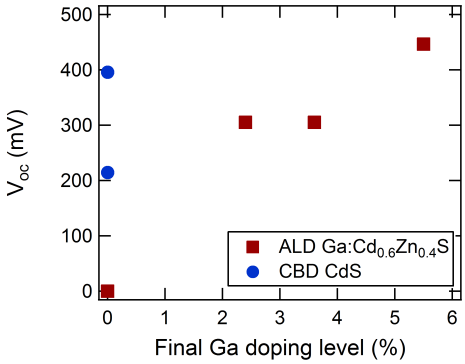

Figure S9: Increasing the Ga-doping in our $Cd_{0.6}Zn_{0.4}S$ resulted in a doubling of the maximum V_{OC} (out of a set of 5 devices at each composition/doping level) compared to a CBD CdS control. However, overall device efficiency remained low, due to insufficient J_{SC} and FF. Also included is the CBD CdS device V_{OC} from Fig. S3, made using a different $CuSbS_2$ absorber.